Journal of Pharmaceutical Sciences 106 (2017) 973-981

Contents lists available at ScienceDirect

Journal of Pharmaceutical Sciences

journal homepage: www.jpharmsci.org

Drug Discovery—Development Interface

Structural Analysis of Heparin-Derived 3-*O*-Sulfated Tetrasaccharides: Antithrombin Binding Site Variants

Yin Chen [1, 2, 3, 4, 5, *], Lei Lin [2, 3, 4, 5], Isaac Agyekum [6], Xing Zhang [2, 3, 4, 5], Kalib St. Ange [2, 3, 4, 5], Yanlei Yu [2, 3, 4, 5], Fuming Zhang [2, 3, 4, 5], Jian Liu [7], I. Jonathan Amster [6], Robert J. Linhardt [2, 3, 4, 5, *]

[1] *College of Food and Pharmacy, Zhejiang Ocean University, Zhoushan, Zhejiang 316000, China*
[2] *Department of Chemistry and Chemical Biology, Center for Biotechnology and Interdisciplinary Studies, Rensselaer Polytechnic Institute, Troy, New York 12180*
[3] *Department of Biology, Center for Biotechnology and Interdisciplinary Studies, Rensselaer Polytechnic Institute, Troy, New York 12180*
[4] *Department of Chemical and Biological Engineering, Center for Biotechnology and Interdisciplinary Studies, Rensselaer Polytechnic Institute, Troy, New York 12180*
[5] *Department of Biomedical Engineering, Center for Biotechnology and Interdisciplinary Studies, Rensselaer Polytechnic Institute, Troy, New York 12180*
[6] *Department of Chemistry, University of Georgia, Athens, Georgia 30602*
[7] *Division of Chemical Biology and Medicinal Chemistry, Eshelman School of Pharmacy, University of North Carolina, Chapel Hill, North Carolina 27599*

ARTICLE INFO

Article history:
Received 8 October 2016
Revised 16 November 2016
Accepted 29 November 2016
Available online 20 December 2016

Keywords:
antithrombin-binding site
heparin-derived tetrasaccharides
anticoagulant activity
heparin lyase
structure-activity relationship

ABSTRACT

Heparin is a polysaccharide that is widely used as an anticoagulant drug. The mechanism for heparin's anticoagulant activity is primarily through its interaction with a serine protease inhibitor, antithrombin III (AT), that enhances its ability to inactivate blood coagulation serine proteases, including thrombin (factor IIa) and factor Xa. The AT-binding site in the heparin is one of the most well-studied carbohydrate-protein binding sites and its structure is the basis for the synthesis of the heparin pentasaccharide drug, fondaparinux. Despite our understanding of the structural requirements for the heparin pentasaccharide AT-binding site, there is a lack of data on the natural variability of these binding sites in heparins extracted from animal tissues. The present work provides a detailed study on the structural variants of the tetrasaccharide fragments of this binding site afforded following treatment of a heparin with heparin lyase II. The 5 most commonly observed tetrasaccharide fragments of the AT-binding site are fully characterized, and a method for their quantification in heparin and low-molecular-weight heparin products is described.

Introduction

Despite having been discovered 100 years ago by a medical student in 1916,[1] the structure of the clinical anticoagulant heparin is still not completely understood.[2] Heparin (and the related glycosaminoglycan heparan sulfate) is a linear polysaccharide comprised of 1→4-glycosidically linked alternating uronic acid (UA), α-L-iduronic acid (IdoA) or β-D-glucuronic acid (GlcA), and α-D-glucosamine (GlcN) residues.[2] The UA residues can be substituted with 2-*O*-sulfogroups and the GlcN residues can be unsubstituted or substituted with *N*-sulfo or *N*-acetyl groups and 3-*O*-sulfo, and/or 6-*O*-sulfo group substituted.[2]

These sulfo group substitutions take place within the Golgi during biosynthesis through the action of sulfotransferases (STs).[3,4] In mammals, there are multiple isoforms of *N*-deacetylase, *N*-sulfotransferases (NDSTs), 3-*O*-sulfotransferases (3OSTs), and 6-*O*-sulfotransferases (6OSTs) but only single isoforms of 2-*O*-sulfotransferase

Abbreviations used: AT, antithrombin III; UA, uronic acid; IdoA, iduronic acid; GlcA, β-D-glucuronic acid; GlcN, α-D-glucosamine; STs, sulfotransferases; NDST, *N*-sulfotransferase; 3OST, 3-*O*-sulfotransferase; 6OST, 6-*O*-sulfotransferase; 2OST, 2-*O*-sulfotransferase; LMWH, low-molecular-weight heparin; MS, mass spectrometry; MS/MS, tandem MS; NMR, nuclear magnetic resonance spectroscopy; HPLC, high-performance liquid chromatography; ΔUA, deoxy-α-L-*threo*-hex-4-enopyranosyluronic acid; SAX, strong anion exchange; S, sulfo; CID, collisionally induced dissociation; EDD, electron-detachment dissociation; HSQC, heteronuclear single quantum coherence; COSY, ^{1}H-^{1}H homonuclear correlation spectroscopy; TOCSY, total correlation spectroscopy.

The authors declare no competing financial interest.

The authors Yin Chen and Lei Lin contributed equally.

This article contains supplementary material available from the authors by request or via the Internet at http://dx.doi.org/10.1016/j.xphs.2016.11.023.

* *Correspondence to:* Yin Chen (Telephone: 86-580-255-4781; Fax: 255-4781) and Robert J. Linhardt (Telephone: 1-518-276-3404; Fax: 276-3405).

E-mail addresses: mojojo1984@163.com (Y. Chen), linhar@rpi.edu (R.J. Linhardt).

http://dx.doi.org/10.1016/j.xphs.2016.11.023
0022-3549/

(2OST).[4] The action of 3OST is believed to be the last step in heparin biosynthesis and the action of different 3OST isoforms appears to impart specialized functions to heparin chains.[5-7] For example, the action of 3OST-1 is responsible for the biosynthesis of anticoagulant-active heparin whereas the action of 3OST-5 results in the biosynthesis of nervous tissue heparan sulfate that serves as a coreceptor for herpes simplex virus[5] and multiple isoforms are involved in the biosynthesis of follicular heparan sulfate important in ovulation.[7]

Heparin's anticoagulant activity depends on its interaction with the serine protease inhibitor, antithrombin III (AT), which on binding to heparin undergoes a conformational change that enhances its ability to irreversibly inhibit coagulation serine proteases, including thrombin and factor Xa.[8] Heparin-AT binding is one of the most well studied carbohydrate-protein interactions and depends on a specific type of pentasaccharide sequence[9] within heparin that contains a 3-*O*-sulfo group in its central GlcN residue.[10] There is some reported structural variability in this pentasaccharide sequence[11,12] particularly associated with heparins from different tissues or species.[13]

Pharmaceutical heparins are currently extracted from the tissues of food animals that are rich in the mast cells that biosynthesize heparin.[14] The major source of heparin today is porcine intestinal mucosa, but in the past, heparin has been prepared from bovine lung and bovine intestinal mucosa.[15] Moreover, there is current interest in the chemoenzymatic synthesis of non−animal-sourced heparins.[16] In 2007, pharmaceutical heparin was contaminated with a toxic semisynthetic glycosaminoglycan, oversulfated chondroitin sulfate.[17] Furthermore, there is a growing concern that much of the heparin comes from a single species and is sourced from a single country.[18] Thus, the US Food and Drug Administration has recommended the development of other heparin sources to address the current fragile supply chain for this critical drug.[18]

The present study examines the structural variability of the AT-binding sites within heparin. Heparins from different sources and low-molecular-weight heparins (LMWHs), prepared through the controlled depolymerization of pharmaceutical heparin,[19,20] were depolymerized through exhaustive treatment with the enzyme heparin lyase II.[21] The resulting resistant tetrasaccharides containing 3-*O*-sulfo groups[22] were isolated, purified, and characterized using mass spectrometry (MS), tandem MS (MS/MS), and nuclear magnetic resonance spectroscopy (NMR). Five tetrasaccharide structures were determined, which provide an important insight into the structural variability of the AT-binding site within pharmaceutical heparins. A high performance liquid chromatography (HPLC)-MS assay was also developed that allows quantification of these 3-*O*-sulfo group tetrasaccharides.

A detailed understanding of the possible biosynthetic variability in the AT-binding site structure is necessary for the development of a detailed structure-activity relationship. The chemically synthesized drug Arixtra® (fondaparinux) has been successfully used as a highly selective anticoagulant for over 2 decades.[23] The structure of Arixtra® is based on a single structural variant of the AT-pentasaccharide binding site.[10] Chemoenzymatic synthesis has reduced the number of synthetic steps for the efficient synthesis of this and other variant AT-binding sites.[24,25] This study is aimed at increasing the number of targets for directed chemoenzymatic synthesis.

Results and Discussion

Preparation of Tetrasaccharides From Porcine Intestinal Mucosal Heparin

Heparin was treated exhaustively with recombinantly expressed heparin lyase II.[26] This enzyme is known to show the least selectivity among the 3 *Flavobacterial* heparin lyases[21,27,28] cleaving both highly sulfated and undersulfated domains within heparin.[27,28] Despite its broad specificity, certain tetrasaccharides are resistant to heparin lyase II digestion.[22] While fully sulfated, hexasulfated tetrasaccharide, ΔUA2S (1→4) GlcNS6S (1→4) IdoA2S (1→4) GlcNS6S (where ΔUA is deoxy-α-L-*threo*-hex-4-enopyranosyluronic acid), can be cleaved by heparin lyase II into 2 molecules of ΔUA2S (1→4) GlcNS6S. This step required long reaction time and large amount of enzyme. In contrast, tetrasaccharides containing a 3-*O*-sulfo group on their reducing-end GlcN residue are completely resistant to heparin lyase II digestion.[22] Thus, as expected, exhaustive digestion with heparin lyase II afforded primarily disaccharides together with a minor amount of heparin lyase II−resistant tetrasaccharides. A Bio-Gel P2 size-exclusion column afforded a good separation of disaccharides from resistant tetrasaccharides and heparin lyase II protein (Supplementary Fig. S1).

Further purification of the tetrasaccharides was carried out by semipreparative strong anion exchange (SAX)-HPLC (Fig. 1). Initially, a gradient elution was used to remove other products from a mixture containing primarily tetrasaccharides. The tetrasaccharide-containing mixture was recovered, desalted, and reapplied using an optimized gradient to obtain the individual tetrasaccharide. Approximately 25 prominent peaks were examined by MS after desalting. From the MS, we found that some peaks contained disaccharides or trisaccharides. The tetrasaccharide-containing peaks were repurified by SAX-HPLC. As expected, exhaustive heparin lyase II treatment failed to digest some tetrasaccharides that did not contain 3-*O*-sulfo groups, such as the hexasulfated tetrasaccharide.[29] Retreatment of these tetrasaccharides, however, showed that they were sensitive to heparin lyase II. Only 5 tetrasaccharides were completely resistant to heparin lyase II and their purity was assessed to be >90% by analytical SAX-HPLC (Supplementary Fig. S2). These all most likely are afforded as the direct result of heparin biosynthesis because the

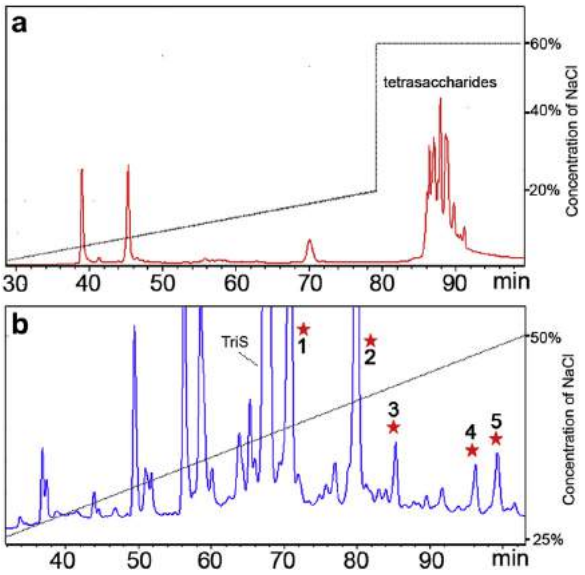

Figure 1. SAX-HPLC of the crude tetrasaccharides recovered from size-exclusion chromatography (Supplementary Fig. S1). (a) A linear gradient of mobile phase B ($t_{0\text{-}20}$ min 0%; $t_{20\text{-}80}$ min 0%-20%; $t_{80\text{-}120}$ min 60%) was applied to separate the tetrasaccharides from other components of the mixture. The structures of tetrasaccharides 1-5 are shown in Figures 2 and 3. The structure of TriS is ΔUA2S-GlcNS6S. (b) After desalting the tetrasaccharides, the sample was again applied to the column using an optimized gradient of mobile phase B ($t_{0\text{-}100}$ min 25%-50%) to recover individual tetrasaccharides. Detection relied on UV absorbance at 232 nm.

conditions, used in the preparation of heparin and these tetrasaccharides, are considerably milder than the conditions required for the degradative loss of sulfate groups from heparin.[30]

Characterization of the Tetrasaccharides by MS

MS analysis provided initial structural information on 5 heparin lyase II−resistant tetrasaccharides (Supplementary Figs. S3a-S3e, tetrasaccharides **1**-**5**). MS analysis showed the basic structures of the tetrasaccharides (Table 1): tetrasaccharide 1 (**1**) with the molecular mass of 956.07 was composed of ΔUA-GlcN-UA-GlcN + Ac + $3SO_3$; tetrasaccharide 2 (**2**) with the molecular mass of 1035.01 was composed of ΔUA-GlcN-UA-GlcN + Ac + $4SO_3$; tetrasaccharide 3 (**3**) with the molecular mass of 1072.97 was composed of ΔUA-GlcN-UA-GlcN + $5SO_3$; tetrasaccharide 4 (**4**) with the molecular mass of 1115.01 was composed of ΔUA-GlcN-UA-GlcN + Ac + $5SO_3$; and tetrasaccharide 5 (**5**) with the molecular mass of 1152.95 was composed of ΔUA-GlcN-UA-GlcN + $6SO_3$. The retention times on SAX-HPLC increased with the total number of sulfo (S) groups.

MS/MS analysis was next used to examine the structure of each tetrasaccharide (Fig. 2). Negative mode electrospray ionization (ESI) of each tetrasaccharide produced abundant multiply charged precursor ions allowing for efficient activation of their molecular ions. We have considered mostly sodium-adducted precursor ions for this analysis to reduce the decomposition of the labile sulfate groups on the tetrasaccharides[31] during ion activation.

The MS/MS of **1** shows the annotated structure for collisionally induced dissociation (CID) fragmentation of the $[M\text{-}5H+2Na]^{3-}$ precursor ion at *m/z* 332.3416 (Fig. 2a). This ionized state allows for all the ionizable protons to be deprotonated. The 6-*O*-sulfogroup on the internal N-acetylglucosamine (GlcNAc) residue is assigned with a combination of both cross-ring and glycosidic product ions. The mass difference between C_1/B_1 and C_2/B_2[32] identifies a sulfo group on the GlcNAc whereas the mass difference between product ions $^{2,4}A_2$ and $^{0,2}A_2$ or $^{0,3}A_2$ and B_2 specifically locates the sulfo group at the 6-*O*-position. The 2 sulfo groups on the reducing end GlcN residue are assigned using the masses of Y_1 or Z_1. The 3-*O*-sulfo on the GlcNS is assigned using the mass difference between the C_3 and $^{2,4}A_4$ ions respectively.

The MS/MS of **2** produced abundant $[M\text{-}6H+2Na]^{4-}$ *m/z* 268.9936 for electron-detachment dissociation (EDD) activation. Again with the aid of Na/H, we are able to ionize all ionizable protons. Good structural coverage was observed allowing assignment of the structure of the compound (Fig. 2b). The mass difference between B_1 or C_1 and B_2 and C_2 identifies a sulfo group on the internal GlcNAc. The mass difference between product ions $^{0,3}A_2$ and C_2 assigns the 6-*O*-sulfo group on the GlcNAc. The GlcN residue at the reducing end containing 3 sulfo groups is confidently assigned with glycosidic product ion Y_1. Cross-ring ions $^{1,4}X_0$ and $^{0,2}X_0$ specifically locates the 6-*O*- and *N*-sulfo groups.

The MS/MS of **3** relied on CID product ion assignment (Fig. 2c). CID activation of the $[M\text{-}6H+2Na]^{4-}$ at *m/z* 278.4802 produced enough glycosidic and cross-ring cleavages for structural analysis. Accurate mass difference between glycosidic ions C_1 and C_2 locates 2 sulfo groups on the internal GlcN residue at the *N*- and 6-*O*-positions. The exact positions of these sulfo groups are assigned using the mass difference between products ions $^{2,4}A_2$ and $^{0,2}A_2$, and B_2 and $^{0,2}A_2$, respectively. The mass of the glycosidic cleavage Y_1 locates 3 sulfo groups on the reducing end GlcN. The 3-*O*-sulfo group on the reducing end GlcN is confirmed by accurate mass difference between fragment ions Y_1 and $^{2,4}X_0$. The mass of $^{2,4}X_0$ can also confirm the presence of 2 sulfo groups at the 6-*O*- and *N*-positions with $^{0,2}A_4$ specifically locating the *N*-sulfo group.

The MS/MS of **4**, a pentasulfated tetrasaccharide, is shown in Figure 2d. The molecular ion $[M\text{-}6H+2Na]^{4-}$ at *m/z* 288.9830 was subjected to CID activation and generated structurally informative ions for assigning the structure. The mass of glycosidic ions B_1 and C_1 provided evidence for a nonreducing end−sulfated UA (ΔUA2S). The mass difference between B_2/C_2 and B_1/C_1 identified a sulfo group on the internal GlcNAc. This sulfo group was on the 6-*O*-position as confirmed with the accurate mass difference between cross-ring product ions $^{0,2}A_2$ and $^{2,4}A_2$. Again, we assigned the reducing end GlcN residue having 3 sulfo groups from Z_1 and Y_1. The exact positions of the sulfo groups are confirmed with multiple cross-ring cleavages as shown in Figure 2d.

The MS/MS of **5**, a hexasulfated tetrasaccharide, is shown in Figure 2e. The structure of **5** was determined by combining fragment ions from EDD and CID activation of the $[M\text{-}5H + Na]^{4-}$ *m/z* 292.9730. The 2-*O*-sulfo nonreducing end UA is assigned from the mass of either the B_1 or C_1 fragment. Accurate mass difference between the C_2 or B_2 and C_1 or B_1 locates 2 sulfo groups on the internal GlcN residue. We are able to eliminate the possibility of 3-*O*-group on this GlcN unit from the accurate mass of $^{2,4}X_2$ fragment, which allows the assignment of the 2 sulfo groups at the 6-*O*- and *N*- positions. The sulfo group on the nitrogen is further confirmed by subtracting the mass of the $^{0,2}A_2$ ion from the B_2 ion. Using both CID and EDD, we confirmed the presence of the reducing end GlcN residue a GlcNS3S6S from cleavages Z_1 or Y_1. We have included a comprehensive mass list (*m/z* intensity) for all the tetrasaccharides in the accompanying Supplementary Material Tables S1-S6.

Characterization of the Tetrasaccharides by NMR Spectroscopy

NMR spectroscopy is essential for assigning the stereochemistry of internal UA residue epimeric form within each tetrasaccharide and also confirms the positions of the *N*-acetyl, *N*- and *O*-sulfo groups (Figs. 3a-3e). The 4 signals between 4.5 and 5.5 ppm were characteristic of the anomeric protons of the tetrasaccharides A, B, C, and D residue, that is, $_{\text{non-reducing end}}A \rightarrow B \rightarrow C \rightarrow D_{\text{reducing end}}$. The singlet signal at ~2.0 ppm was assigned to the methyl protons of *N*-acetyl group of the GlcNAc residue. The signal, which had the largest chemical shift at ~5.7 ppm and correlated to the carbon signal at 107 ppm in heteronuclear single quantum coherence (HSQC) spectra (Supplementary Figs. S4a-S4e), was assigned to the H4 proton of the ΔUA residue at the nonreducing end of each tetrasaccharide (residue A). The signals, located between 3.2 and 4.5 ppm, were assigned using ^1H-^1H homonuclear correlation spectroscopy (COSY) to determine connectivity around each ring. Beginning with the furthest downfield signal at 5.7 ppm assigned to the H4 of ΔUA connectivity to H3, H2 and H1 of the nonreducing end ΔUA in each tetrasaccharide were established (Figs. 4a-4e). In the HSQC spectra, the anomeric carbon at ~91 ppm showing the

Table 1
Structures and Mass Spectral Properties of Tetrasaccharides

Parameters	1	2	3	4	5
Structural features	ΔUA→GlcN→UA→GlcN + Ac+$3SO_3$	ΔUA→GlcN→UA→GlcN+Ac+$4SO_3$	ΔUA→GlcN→UA→GlcN+$5SO_3$	ΔUA→GlcN→ UA→GlcN+Ac+$5SO_3$	ΔUA→GlcN→UA→GlcN+$6SO_3$
Ions (2-)	477.03	517.01	535.98	557.00	575.96
Molecular mass	956.07	1035.01	1072.97	1115.01	1152.95

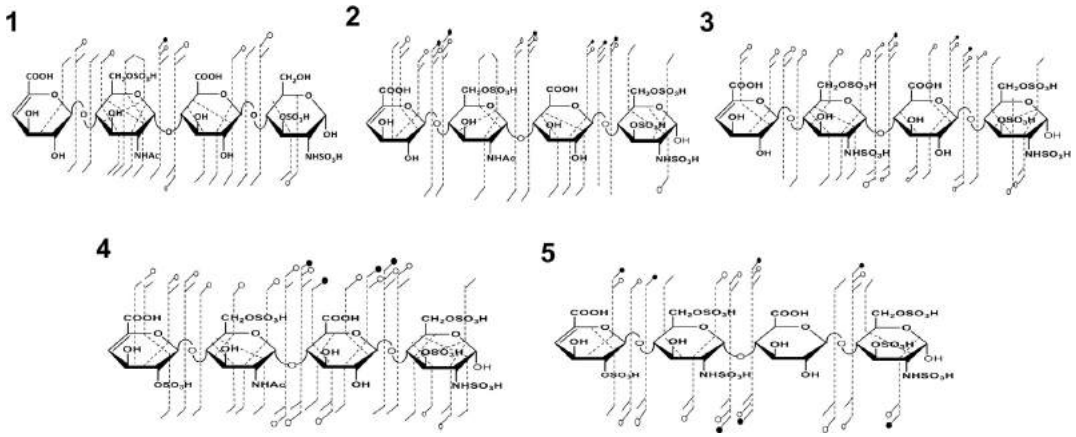

Figure 2. MS/MS structural annotations for CID of **1** ΔUA-GlcNAc6S-GlcA-GlcNS3S; EDD of **2** ΔUA-GlcNAc6S-GlcA-GlcNS3S6S; CID of **3** ΔUA-GlcNS6S-GlcA-GlcNS3S6S; CID of **4** ΔUA2S-GlcNAc 6S-GlcA-GlcNS3S6S; and CID/EDD of **5** ΔUA2S-GlcNS6S-GlcA-GlcNS3S.

smallest chemical shift of the 4 anomeric carbons is the C1 of the GlcN residue at the reducing end. The anomeric proton (H1) correlating is at the reducing end GlcN residue (residue D). The most upfield anomeric signal at 4.5 ppm in the ^{1}H NMR, having a coupling constant of 8 Hz, correlates to the C1 signal at ~100.5 ppm. This signal is the characteristic of a β-configured GlcA residue in heparin, confirming the epimeric structure of the internal UA (residue C). By confirming 3 of the anomeric protons, the remaining 1 must correspond to the internal GlcN residue (residue B). Using COSY and total correlation spectroscopy (TOCSY), all the remaining

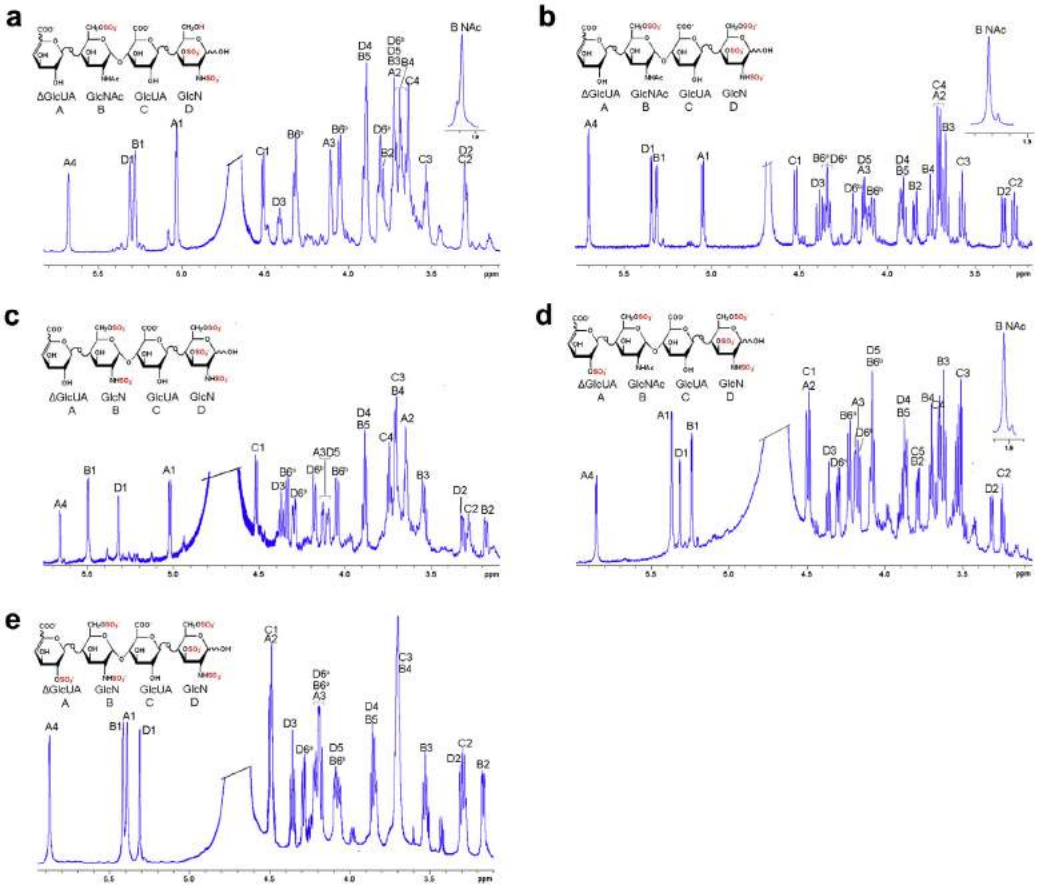

Figure 3. Structures and 1D ^{1}H NMR spectra of **1**-**5** are shown in panels (a-e) respectively.

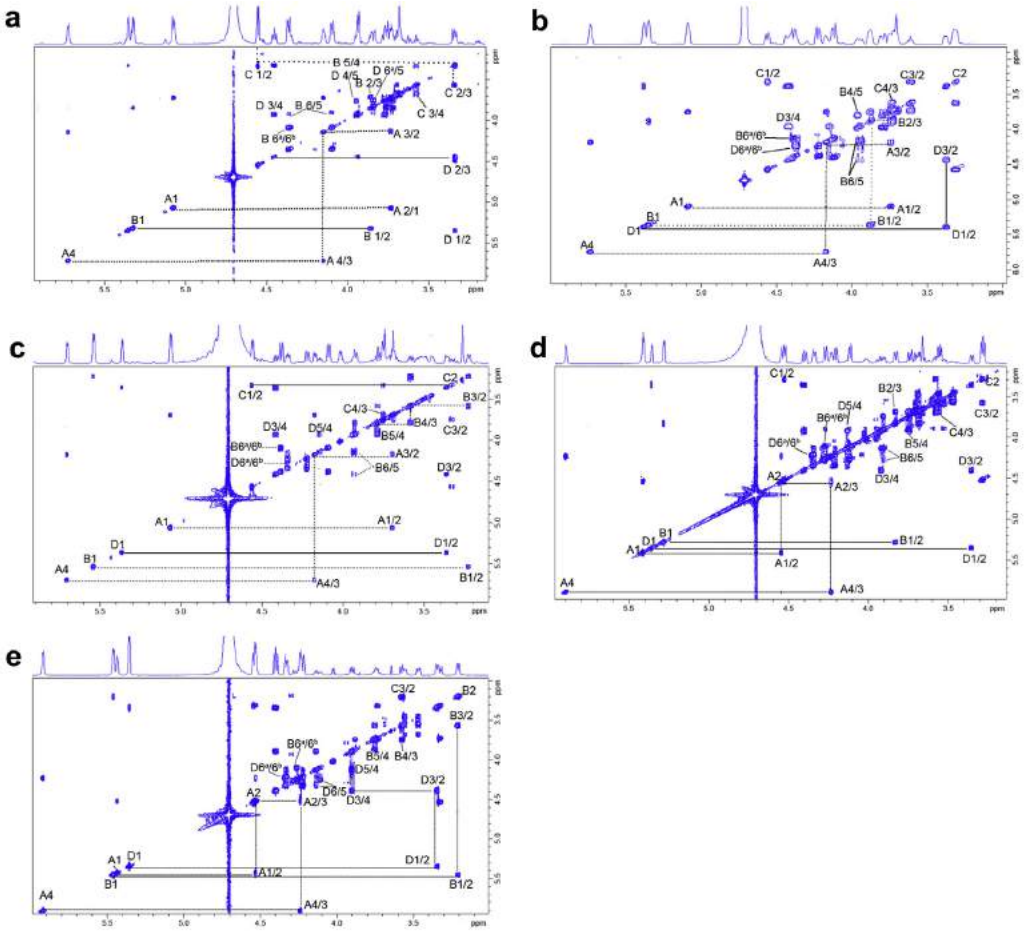

Figure 4. The COSY spectra of **1**-**5** are shown in panels (a-e) respectively.

saccharide ring protons could be assigned through their connectivity to their H1 protons (Supplementary Figs. S5a-S5e). The fully assigned ^{1}H and ^{13}C NMR data are presented in Table 2.

Tetrasaccharides **1**-**5** each showed 4 anomeric protons corresponding to nonreducing end ΔUA (A), internal GlcN (B), internal GlcA (C), and reducing end GlcN (D). On account of anomerization of the reducing end saccharide, both α- and β-anomeric forms are possible. In all 5 heparinase II–resistant tetrasaccharides, the reducing end GlcN is only found in the α-configuration. This suggests that all of the terminal GlcN residues were substituted with *N*-sulfo groups, fixing these residues in the α-configuration. NMR analysis of heparin shows that substitution with an *N*-sulfo group results in a large upfield shift of the H2 of the GlcN residue when compared to substitution with an *N*-acetyl group. This was clearly observed in the spectrum of **1**, where the H2 of internal GlcNAc residue was at 3.81 ppm, similar to the GlcNAcH2 signal reported for heparin, whereas the H2 of the reducing end GlcNS was shifted upfield to 3.29 ppm. This evidence also supports the presence of an *N*-sulfo reducing end GlcN residue. Next, the remaining signals of reducing end GlcN (D) and the internal GlcN (B) residues were compared. The chemical shifts of the reducing end GlcNSH6$_{a,b}$ and C6 were 3.81, 3.73 ppm and 59.8 ppm, respectively, whereas that of internal GlcNAcH6$_{a,b}$ and C6 were 4.32, 4.05 ppm and 65.8 ppm, respectively. The downfield shifts of these signals of the internal GlcNAc indicate the presence of a 6-*O*-sulfo group. The H3 of the reducing end GlcNS residue was shifted downfield to 4.43 ppm compared to the H3 of internal GlcNAc residue at 3.72 ppm, indicating the 3-*O*-sulfo group was on GlcNS residue at the reducing end. Based on these analyses, the structure of **1** was found to be consistent with ΔUA-GlcNAc6S-GlcA-GlcNS3S.

The 1D and 2D COSY spectra of **2** are presented in Figs. 3b and 4b. The critical characteristics of **2** were similar to **1**. No significant differences were observed except for the downfield shift in the H6$_{a,b}$ of the reducing end GlcNS (D) by 0.53 and 0.45 ppm, and the chemical shifts of H6 and C6 were similar to those of the internal 6-*O*-sulfoGlcNS (B). So both the GlcNS residues of **2** are substituted with 6-*O*-sulfo groups. The structure of **2** was found to be consistent with ΔUA-GlcNAc6S-GlcA-GlcNS3S6S.

The 1D spectrum of **3** showed no resonance for the methyl protons of the acetamido group (Fig. 3c), indicating both GlcN (B) and GlcN (D) were substituted with *N*-sulfo groups. The chemical shift of H2 of GlcNS (B) was 3.18 ppm, consistent with a GlcNS residue. The structure of **3** was found to be consistent with ΔUA-GlcNS6S-GlcA-GlcNS3S6S.

The anomeric proton of the ΔUA (A) residue in **4** was shifted downfield from 5.02 ppm to 5.37 ppm (Fig. 3d). In contrast, the anomeric carbon of the ΔUA (A) residue was shifted upfield from 100.7 ppm to 97.0 ppm (Supplementary Fig. S4d). In addition, the H2 signal of the ΔUA (A) residue was shifted to 4.5 ppm from 3.65

Table 2
Chemical Shifts (δ ppm) and Coupling Constants (in Hz) of Tetrasaccharides

Residues	1	2	3	4	5
ΔUA (A)					
H1	5.03(6.0)	5.05(6.2)	5.02(6.3)	5.37(2.7)	5.36(1.6)
C1	100.4	100.9	100.7	97.0	96.7
H2	3.69	3.70	3.65	4.50	4.49
C2	70.2	70.0	70.5	74.4	74.5
H3	4.12	4.19	4.13	4.16	4.20
C3	66.7	66.6	67.0	62.3	62.6
H4	5.68(1.8)	5.70(3.6)	5.66(3.0)	5.85(4.9)	5.87(3.9)
C4	107.3	107.6	107.4	107.6	106.3
GlcN (B)					
H1	5.28(3.8)	5.31(3.7)	5.49(3.6)	5.24(3.9)	5.42(3.3)
C1	96.5	96.6	96.9	96.8	97.6
H2	3.81	3.84	3.18	3.79	3.17
C2	53.2	53.3	57.5	53.0	57.4
H3	3.72	3.70	3.55	3.62	3.52
C3	75.7	76.7	69.4	76.6	69.1
H4	3.70	3.72	3.71	3.70	3.7
C4	76.1	76.7	77.4	77.9	77.6
H5	3.89	3.91	3.88	3.87	3.85
C5	68.9	68.8	68.3	68.6	68.4
$H6_{a,b}$	4.32,4.05	4.35,4.07	4.34,4.45	4.3,4.07	4.19,4.06
C6	65.8	65.8	65.6	66.0	65.9
NAc	1.91/21.2	1.87/21.6	–	1.93/21.3	–
GlcA (C)					
H1	4.51(7.9)	4.52(8.0)	4.52(7.8)	4.48(8.0)	4.5(7.7)
C1	100.3	100.8	100.8	100.9	101.1
H2	3.29	3.28	3.28	3.25	3.28
C2	73.0	73.5	72.5	73.3	72.3
H3	3.53	3.56	3.71	3.52	3.7
C3	76.4	76.4	76.0	76.1	75.7
H4	3.64	3.69	3.75	3.65	ND
C4	77.4	77.8	76.7	76.6	
H4	ND	ND	ND	ND	ND
C5					
GlcN (D)					
H1	5.32(3.1)	5.34(3.3)	5.32(3.0)	5.32(3.2)	5.31(3.2)
C1	91.0	91.1	91.1	90.8	91.0
H2	3.29	3.34	3.32	3.31	3.30
C2	56.7	57.3	56.8	56.5	56.6
H3	4.43	4.38	4.37	4.36	4.36
C3	75.6	75.6	75.8	75.2	75.1
H4	3.90	3.92	3.88	3.89	3.84
C4	73.0	73.0	73.3	73.1	73.3
H5	3.72	4.08	4.1	4.08	4.09
C5	68.9	68.8	69.3	68.1	68.8
$H6_{a,b}$	3.81,3.73	4.34,4.18	4.3,4.18	4.22,4.0	4.29,4.18
C6	59.8	65.8	66.1	65.8	66.1
NAc	–	–	–	–	–

ND, not detected.

ppm, almost completely overlapped with the H1 proton of GlcA (C). These spectral properties are consistent with the 2-*O*-sulfo group-substitution of the ΔUA (A) residue. Thus, the structure of **4** was found to be consistent with ΔUA2S-GlcNAc6S-GlcA-GlcNS3S6S.

The MS and 1D ^{1}H NMR spectra of **5** (Fig. 3e) showed that it had no acetyl group. The H2 of ΔUA (A) residue also overlapped with anomeric proton of GlcA at 4.5 ppm consistent with a nonreducing terminal ΔUA2S. The HSQC spectrum (Supplementary Fig. S4e) showed both the GlcNS (B) and GlcNS (D) residues were substituted with 6-*O*-sulfo groups, having chemical shifts for H6 and C6 of >4.0 ppm and 65 ppm, respectively. The H3 of the reducing end GlcNS (D) residue of **5** was consistent with the presence of a 3-*O*-sulfo group. Thus, the structure of **5** was found to be consistent with ΔUA2S-GlcNS6S-GlcA-GlcNS3S6S.

All 5 tetrasaccharides clearly had 3-*O*-sulfo group substitution of the reducing end GlcNS residue, consistent with the known specificity of heparin lyase II resistance.[22,27,28] The ΔUA at the nonreducing end was either unsubstituted or substituted with 2-*O*-sulfo groups again consistent with the known substrate specificity of heparin lyase II.[22,27,28] The internal UA was GlcA and no sulfation of this residue was observed. The assignment of the internal GlcA was challenging, as we were unable to fully assign this residue. In the COSY, the continuous cross-peaks stopped at H3/H4 and no cross-peak for H4/H5 was observed. In the TOCSY, no H5 signal could be found and only correlation peaks for H1/H2, H1/H3, and H1/H4 were found. This failure might result from the close chemical shifts for H4/H5 and C4/C5. These 2 signals are nearly completely overlapped. The internal GlcN residue could be substituted with *N*-acetyl or *N*-sulfo group but always contained a 6-*O*-sulfo group.

Standard Curve of Tetrasaccharide Analysis

The most abundant disaccharide formed, when heparin is digested with heparin lyase II, is the trisulfated disaccharide, ΔUA2S-GlcNS6S. This disaccharide has a ΔUA2S nonreducing terminal residue with a maximum absorbance at 232 nm. The 5 heparin lyase II–resistant 3-*O*-sulfo group–substituted tetrasaccharides had either a ΔUA or a ΔUA2S residue, with the same absorbance maximum, and between 3 and 6 sulfates. Thus, we selected ΔUA2S-GlcNS6S as an external standard to quantify these 5 tetrasaccharides. At the range of 0.02 mg/mL and 0.2 mg/mL, the peak areas of these 5 tetrasaccharides showed good linearity between peak area and molar concentration.

The composition of tetrasaccharides having 3-*O*-sulfo groups was different in heparin samples. Thus, tetrasaccharide standards with different ranges of concentration were prepared based on the approximate content found in pharmaceutical porcine intestinal heparin (**1**: 64, 128, 192, 256, and 320 ng; **2**:128, 256, 384, 512, and 640 ng; **3**: 64, 128, 50, 192, 256, and 320 ng; **4**: 16, 32, 48, 64, and 80 ng; **5**: 64, 128, 50, 192, 256, and 320 ng). These standard mixtures were analyzed by reversed-phase ion pair (RPIP)-HPLC-MS to evaluate both the sensitivity and the linearity of tetrasaccharide amount and the peak intensities using extracted ion chromatography. The 5 tetrasaccharides showed complete separation (Supplementary Fig. S6). The integrated tetrasaccharide peak areas show good linearity to their amounts (Supplementary Fig. S7). The 5 tetrasaccharides had different ionization efficiencies in an ESI source. Tetrasaccharide **3** showed a greater ionization efficiency, which is reflected by the high slope of its standard curve. Tetrasaccharide **5** with 6 sulfo groups showed the lowest ionization efficiency under the same experimental conditions, and **1**, **3**, and **4** showed comparable intermediate ionization efficiency.

Heparin Lyase II–Resistant 3-O-sulfo Tetrasaccharide Content of Various Heparins and LMWHs

Five different heparin samples and 3 different LMWH samples were completely digested using heparin lyase II in triplicate and then analyzed by RPIP-HPLC-MS. All of the 5 resulting 3-*O*-sulfo tetrasaccharides could be detected and quantified by this method. The extracted ion chromatograms showing their tetrasaccharide compositions are presented in Figure 5 (see Supplementary Fig. S8 for the supporting chromatogram). Heparin and LMWH from different sources contained different contents of heparin lyase II–resistant 3-*O*-sulfo tetrasaccharides. The total contents of these 5 tetrasaccharides ranged from 1.0%-7.0%. The 2 porcine intestinal heparins (USP and SPL2) afforded a total of 6.2% and 5.4% 3-*O*-sulfotetrasaccharides. The 3 bovine lung heparins (SPL BL4, Hepar BL2, and Upjohn BL6 had the lowest total tetrasaccharide content ranging from 1.1% to 4.4%. Tetrasaccharide **2** was the most abundant heparin lyase II–resistant 3-*O*-sulfo tetrasaccharide in all the samples except in BL6, which contained tetrasaccharide **5** as its major component. Among the 3 LMWHs, the levels of **1**-**4** were very similar but major differences in the level of **5** were observed.

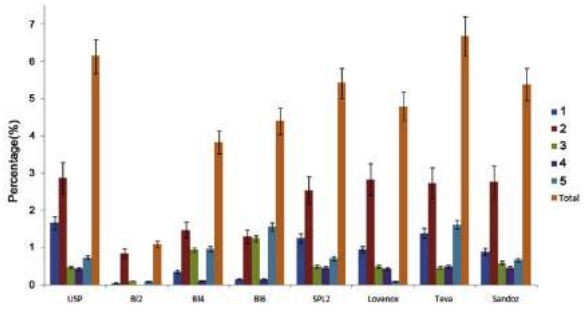

Figure 5. Composition and contents of tetrasaccharides **1**-**5** of heparins and LMWHs (see Supplementary Fig. S8 for the supporting chromatogram).

Correlation Between Anticoagulant Activity and Contents of 3-O-sulfo Group Tetrasaccharides

The anticoagulant activity of heparin, particularly its anti-factor Xa activity, is primarily ascribed to AT-pentasaccharide binding site. The central residue of this pentasaccharide is a 3-*O*-sulfo group−containing GlcN residue. Thus, the 3-*O*-sulfo tetrasaccharide composition and content obtained from heparin lyase II digestion should reflect all the structural variants of AT-binding pentasaccharide, correlating to the anticoagulant activity of heparin samples. These tetrasaccharides can be sensitively analyzed using RPIP-LC-MS (Fig. 6). Only a weak correlation was observed between the anticoagulant activity and the total amount of 3-*O*-sulfo group−containing tetrasaccharide content (not shown). Tetrasaccharide **2**, the most abundant 3-*O*-sulfo group−containing tetrasaccharide, gave the best linear correlation with anticoagulant activity (R^2 = 0.96). These results suggest that different 3-*O*-sulfo group−containing pentasaccharides may exhibit different anticoagulant activities.

Conclusions

The AT-binding site shows a substantial variability in heparins derived from animal tissues (Fig. 7). Five major variants representing >90% of the 3-*O*-sulfo group−containing sequences have been structurally characterized. Both tetrasaccharide **4** and tetrasaccharide **5** are newly discovered compounds obtained from heparin lyase II−digested porcine heparin and to our knowledge

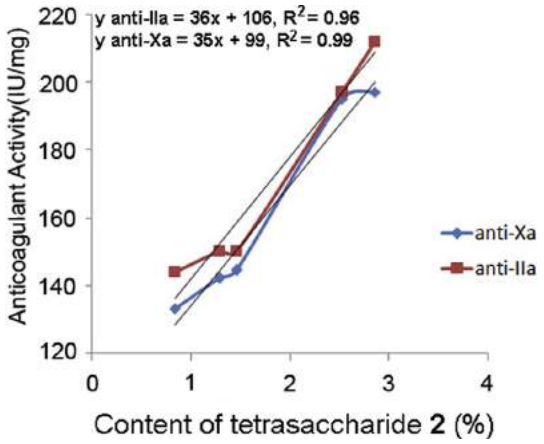

Figure 6. Correlation between anticoagulant activity and the content of 3-*O*-sulfo group−containing tetrasaccharide **2**.

have not been reported by previous publications. In addition, an SAX-HPLC method has been developed that can quantify all the 5 major 3-*O*-sulfo group−containing tetrasaccharides in different heparins. These 5 major variants provide some structure-activity relationship for heparin's anticoagulant activity and provide a deeper understanding of the structural variants of the AT-binding site present within heparin. These sequences show variability in residues A, B, and D. Residue A, lying outside the AT-binding site on its nonreducing end, shows a high level of variability. In this study, it is observed that ΔUA and ΔUA2S, based on the known specificity of heparin lyase II,[33] could correspond to GlcA, IdoA, IdoA2S, and possibly even GlcA2S. The variability of residue B, first reported as a major structural difference between porcine and bovine heparin,[34] can be GlcNS6S or GlcNAc6S. Residue D, containing the critical 3-*O*-sulfo group, can be GlcNS3S6S or GlcNS3S. Interestingly, residue C is invariable and always GlcA. The synthetic pentasaccharide, Arixtra®, is the most highly sulfated version of this binding site, corresponding to tetrasaccharide **5**. It is noteworthy that the content of tetrasaccharide **2**, which correlates best to heparin's anticoagulant activity, contains a lower level of sulfation. This observation may be important in designing synthetic versions of ultra-low-molecular-weight heparins and LMWHs. It is well established that heparin-induced thrombocytopenia, a major side effect associated with the chemical use of heparin, correlates to both the size of the heparin chain and its charge density. This suggests that it might be possible to reduce the level of negative charge within the AT-binding site in the design of new synthetic targets. Finally, the ability to quantify the AT-binding site variants in animal-sourced heparins and LMWHs will assist in our understanding of their biological activities and help us in distinguishing the species and organ source of these products. Future studies will be needed to establish the structure of additional minor 3-*O*-sulfo group−containing tetrasaccharides as well as those present in bovine and ovine heparins.

Materials and Methods

Materials

Heparin lyase II, originating from *Flavobacterium heparinum*, was expressed and purified in *Escherichia coli* (no EC assigned) in our laboratory as described previously. Pharmaceutical heparins were selected having various levels of anticoagulant activity (units of USP activity) from Celsus (Lot: PH-85314), Scientific Protein Laboratories (SPL2, Lot: 1037-3465 and BL4, Lot: 002-139), Hepar (BL2, Lot: 38988C), and Upjohn (BL6, Lot: BU3888B). LMWHs were from Sanofi-Aventis (Lovenox®, enoxaparin, Lot: 4LM92) Teva (enoxaparin, Lot: AB15027), and Sandoz (enoxaparin, Lot: 927791). The ion-pairing reagent tributylamine was purchased from Sigma-Aldrich (St. Louis, MO). All other chemicals were of HPLC grade.

Purification of 3-O-sulfo Tetrasaccharides

Tetrasaccharides containing 3-*O*-sulfo group−substituted GlcN residues at their reducing ends are resistant to heparinase.[35] A 500-mg heparin sample was dissolved in 100 mL digestion buffer (50 mM ammonium acetate, 2 mM calcium chloride) and exhaustively digested by heparin lyase 2 (35 IU, activity against heparin) at 37°C for 6 h. After the reaction finished, the enzyme was removed by centrifugation (8000 × *g*) through a 3-kDa molecular weight cutoff spin column (50 mL). The filtrate that contained the disaccharide and tetrasaccharide products was recovered and freeze-dried.

Buffer salts and most of the disaccharide products were removed by a Bio-Rad P2 column (100 × 2.0 cm) eluted at 0.5 mL/min with distilled water. The first peak from the column contained

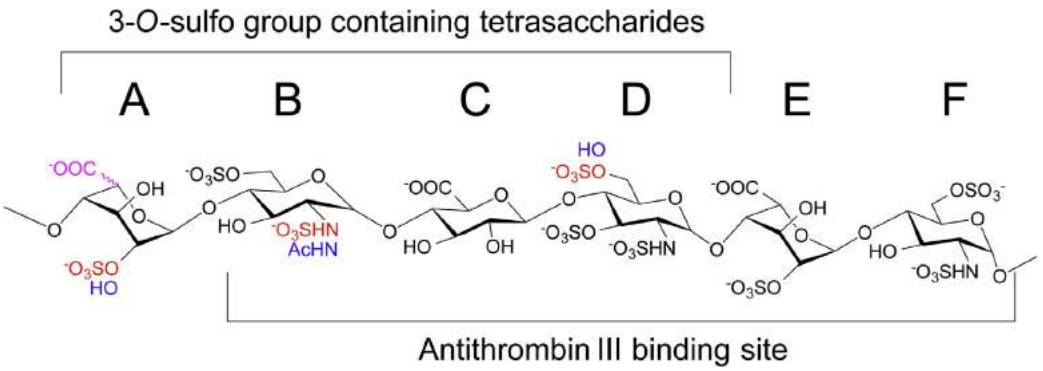

Figure 7. Structural variability of AT-binding site (residues A-F). The substituents shown in red and blue are found within and adjacent to the AT-binding site in heparins derived from animal tissues. The carboxyl group shown in purple can be axial or equatorial for recognition and cleavage by heparin lyase II.

primarily tetrasaccharides as confirmed by MS and was collected and lyophilized. The tetrasaccharide mixture was fractionated on a semipreparative SAX-HPLC column Spherisorb S5 (20 × 250 mm; Waters, Milford, MA). Mobile phase A was water adjusted to pH 3.5 with hydrochloric acid and mobile phase B was 2 M aqueous sodium chloride adjusted to pH 3.5. A stepwise elution was used with linear gradient of mobile phase B ($t_{0\text{-}20}$ min 0%; $t_{20\text{-}80}$ min 0%-20%; $t_{80\text{-}120}$ min 60%) at a flow rate of 4 mL/min. Continuous UV detection was performed at 232 nm. The peaks containing tetrasaccharides eluted from 120 to 140 min. After desalting by Bio-Rad P2 column, the samples were subjected to the second gradient elution: $t_{0\text{-}100}$ min 25%-50% B. The individual peaks eluting were collected and desalted by Bio-Rad P2 column and lyophilized.

Every peak was analyzed using MS, and tetrasaccharide-containing peaks were further purified by repeated separation on the same SAX-HPLC column to obtain pure samples as demonstrated by analytical HPLC. The pure tetrasaccharides were next structurally characterized using NMR and MS/MS. Our final recoveries from 500 mg of heparin were 0.5 mg (5.4%), 0.6 mg (2.7%), 0.2 mg (7.4%), 0.12 mg (2.9%), and 0.12 mg (4.3%) for tetrasaccharide **1**, **2**, **3**, **4**, and **5**, respectively. These recovery yields, based on SAX-HPLC analysis of the starting heparin, range from 2.7% to 7.4% and are low because center cuts of peaks were taken to optimize the purity (>90%) of each oligosaccharide.

Structure Elucidation by NMR

Freeze-dried tetrasaccharide samples were dissolved in 400 μL D_2O (99.96 atom%) and lyophilized 2 times to remove exchangeable protons and transferred to an NMR tube (d = 5 mm). ^{1}H NMR, HSQC NMR, ^{1}H-^{1}HCOSY, and TOCSY were performed on a Bruker 800-MHz NMR spectrometer, and acquisition of the spectra was carried out using Topspin 2.1.6 software. All spectra were acquired at a temperature of 298 K.

Structural Analysis by MS/MS

MS/MS analysis of the 3-*O*-sulfo tetrasaccharides was performed on a 9.4T Bruker Apex Ultra Qh-FTICR instrument (Billerica, MA) fitted with an indirectly heated hollow cathode (HeatWave, Watsonville, CA) for electron generation. Each tetrasaccharide (0.1 mg/mL) in 50:50 methanol/H_2O was infused at a rate of 120 μL/h and ionized by ESI using a metal capillary (Agilent Technologies, Santa Clara, CA, #G2427A). Multiply charged precursor ions were isolated in the external quadruple and activated using CID in the collision cell and EDD in the infinity cell. Also, 512 K points were acquired for each spectra and padded with 1 zero fill and apodized sinebell window. External calibration produced a 5-ppm mass accuracy, and using confidently assigned glycosidic bond cleavage product ions, internal calibration yielded mass accuracy mostly less than 1 ppm. All MS/MS product ions are reported using the Domon and Costello[32]1998 nomenclature.

Enzymatic Digestion of Heparin and LMWH

Heparin and LMWH samples (200 μg) were dissolved in 100 μL of digestion buffer (50 mM ammonium acetate, 2 mM calcium chloride) and digested by heparin lyase II (20 mU) at 37°C for 6 h. The digestion solutions were immediately heated in a 100°C water bath for 5 min to stop the reaction and precipitate proteins. The supernatant was obtained after centrifugation for 15 min (16,000 × g).

Quantity of the Tetrasaccharides by SAX-HPLC

Purified tetrasaccharides were quantified using SAX-HPLC coupling with an analytical Spherisorb S5 (4 × 250 mm; Waters, Milford, MA) at 232 nm. Mobile phase A: 1.8 mM monobasic sodium phosphate, pH 3.0. Mobile phase B: 1.8 mM monobasic sodium phosphate, 1 M sodium perchlorate, pH 3.0. Flow rate: 0.45 mL/min. Gradient: $T_{0\text{-}35}$ min, 30%-65% B; $T_{35\text{-}50}$ min, 65%-85% B. ΔUA2S-GlcNS6S with different concentrations (0.02-0.2 mg/mL) were used as the standard. The linearity was based on amount of peak areas in HPLC.

Reversed-Phase Ion Pair-HPLC-MS

Liquid chromatography-mass spectrometry (LC-MS) analyses were performed on an Agilent 1200 LC/MSD instrument (Agilent Technologies, Wilmington, DE) equipped with a 6300 ion trap. The column used was a Poroshell 120 C18 column (2.1 × 100 mm, 2.7 μm; Agilent Technologies). Eluent A was water/acetonitrile (85:15, v/v), and eluent B was water/acetonitrile (35:65, v/v). Both eluents contained 12 mM tributylamine and 38 mM NH_4OAc with pH adjusted to 6.5 with HOAc. A gradient of solution A for 2 min, followed by a linear gradient of 0% to 30% solution B from 2 to 40 min, and 30% to 60% solution B from 40 to 50 min was used at a flow rate of 120 μL/min. The column effluent entered the source of the ESI-MS for continuous detection by MS. The electrospray interface was set in negative ionization mode with a skimmer potential of −40.0 V, a capillary exit of −40.0 V, and a source temperature of 350°C to obtain the maximum abundance of the ions in a full scan

spectrum (200-1500 Da). Nitrogen was used as a drying (8 L/min) and nebulizing (40 psi) gas.

Calibration

Quantification analysis of 3-*O*-sulfo group−containing tetrasaccharides was performed by using calibration curves constructed by increasing amounts of produced tetrasaccharide standards. The linearity was based on peak intensity in MS. All analyses were performed in triplicate.

Acknowledgments

The work was supported by grants from the National Institutes of Health in the form of Grants HL125371, GM38060, GM103390, GM090127, HL096972, and HL10172. This project was supported by the China Scholarship Council.

References

1. Linhardt RJ. Heparin: an important drug enters its seventh decade. *Chem Industry*. 1991;2:45-50.
2. Linhardt RJ, Claude S. Hudson Award address in carbohydrate chemistry. Heparin: structure and activity. *J Med Chem*. 2003;46:2551-2564.
3. Lindahl U. Biosynthesis of heparin. *Biochem Soc Trans*. 1990;18:803-805.
4. Esko JD, Selleck SB. Order out of chaos: assembly of ligand binding sites in heparan sulfate. *Annu Rev Biochem*. 2002;71:435-471.
5. Moon AF, Edavettal SC, Krahn JM, et al. Structural analysis of the sulfotransferase (3-O-sulfotransferase isoform 3) involved in the biosynthesis of an entry receptor for herpes simplex virus 1. *J Biol Chem*. 2004;279:45185-45193.
6. Edavettal SC, Lee KA, Negishi M, Linhardt RJ, Liu J, Pedersen LC. Crystal structure and mutational analysis of heparan sulfate 3-O-sulfotransferase isoform 1. *J Biol Chem*. 2004;279:25789-25797.
7. De Agostini AI, Dong JC, De Vantéry Arrighi C, et al. Human follicular fluid heparan sulfate contains abundant 3-O-sulfated chains with anticoagulant activity. *J Biol Chem*. 2008;283:28115-28124.
8. Onishi A, St Ange K, Dordick JS, Linhardt RJ. Heparin and anticoagulation, glycosaminoglycans and related disorders. *Front Biosci*. 2016;21:1372-1392.
9. Linhardt RJ, Wang HM, Loganathan D, Bae JH. Search for the heparin antithrombin III-binding site precursor. *J Biol Chem*. 1992;267:2380-2387.
10. Petitou M, van Boeckel CA. A synthetic antithrombin III binding pentasaccharide is now a drug! what comes next? *Angew Chem Int Ed*. 2004;43:3118-3133.
11. Atha DH, Lormeau JC, Petitou M, Rosenberg RD, Choay J. Contribution of monosaccharide residues in heparin binding to antithrombin III. *Biochemistry*. 1985;24:6723-6729.
12. Atha DH, Lormeau JC, Petitou M, Rosenberg RD, Choay J. Contribution of 3-O- and 6-O-sulfated glucosamine residues in the heparin-induced conformational change in antithrombin III. *Biochemistry*. 1987;26:6454-6461.
13. Loganathan D, Wang HM, Mallis LM, Linhardt RJ. Structural variation in the antithrombin III binding site region and its occurrence in heparin from different sources. *Biochemistry*. 1990;29:4362-4368.
14. Horner AA. Rat heparins. A study of the relative sizes and antithrombin-binding characteristics of heparin proteoglycans, chains and depolymerization products from rat adipose tissue, heart, lungs, peritoneal cavity and skin. *Biochem J*. 1986;240:171-179.
15. St Ange K, Onishi A, Fu L, et al. Analysis of heparins derived from bovine tissues and comparison to porcine intestinal heparins. *Clin Appl Thromb Hemost*. 2016;22:520-527.
16. DeAngelis PL, Liu J, Linhardt RJ. Chemoenzymatic synthesis of glycosaminoglycans: re-creating, re-modeling and re-designing nature's longest or most complex carbohydrate chains. *Glycobiology*. 2013;23:764-777.
17. Liu H, Zhang Z, Linhardt RJ. Lessons learned from the contamination of heparin. *Nat Prod Rep*. 2009;26:313-321.
18. Keire D, Mulloy B, Chase C, et al. Diversifying the global heparin supply chain: reintroduction of bovine heparin in the United States? *Pharm Tech*. 2015;39:2-8.
19. Linhardt RJ, Gunay NS. Production and chemical processing of low molecular weight heparins. *Semin Thromb Hemost*. 1999;2:5-16.
20. Bhaskar U, Sterner E, Hickey AM, et al. Engineering of routes to heparin and related polysaccharides. *Appl Microbiol Biotechnol*. 2012;93:1-16.
21. Linhardt RJ. Analysis of glycosaminoglycans with polysaccharide lyases. *Curr Protoc Mol Biol*. 2001;17, 13 B.
22. Xiao Z, Tappen BR, Ly M, et al. Heparin mapping using heparin lyases and the generation of a novel low molecular weight heparin. *J Med Chem*. 2010;54:603-610.
23. Giangrande P. Fondaparinux (Arixtra): a new anticoagulant. *Int J Clin Pract*. 2002;56:615-617.
24. Van Boeckel CA, Petitou M. The unique antithrombin III binding domain of heparin: a lead to new synthetic antithrombotics. *Angew Chem Int Ed*. 1993;32:1671-1690.
25. Xu Y, Masuko S, Takieddin M, et al. Chemoenzymatic synthesis of homogeneous ultralow molecular weight heparins. *Science*. 2011;334:498-501.
26. Li G, Yang B, Li L, Zhang F, Xue C, Linhardt RJ. Analysis of 3-O-sulfo group-containing heparin tetrasaccharides in heparin by liquid chromatography−mass spectrometry. *Anal Biochem*. 2014;455:3-9.
27. Desai UR, Wang HM, Linhardt RJ. Specificity studies on the heparin lyases from Flavobacterium heparinum. *Biochemistry*. 1993;32:8140-8145.
28. Desai UR, Wang H, Linhardt RJ. Substrate specificity of the heparin lyases from Flavobacterium heparinum. *Arch Biochem Biophys*. 1993;306:461-468.
29. Yamada S, Yoshida K, Sugiura M, et al. Structural studies on the bacterial lyase-resistant tetrasaccharides derived from the antithrombin III-binding site of porcine intestinal heparin. *J Biol Chem*. 1993;268:4780-4787.
30. Jandik K, Kruep D, Cartier M, Linhardt RJ. Accelerated heparin stability studies. *J Pharm Sci*. 1996;85:45-51.
31. Kailemia MJ, Li L, Xu Y, Liu J, Linhardt RJ, Amster IJ. Structurally informative tandem mass spectrometry of highly sulfated natural and chemoenzymatically synthesized heparin and heparan sulfate glycosaminoglycans. *Mol Cell Proteomics*. 2013;12:979-990.
32. Domon B, Costello CE. A systematic nomenclature for carbohydrate fragmentations in FAB-MS/MS spectra of glycoconjugates. *Glycoconj J*. 1988;5:397-409.
33. Shaya D, Zhao W, Garron ML, et al. Catalytic mechanism of heparinase II investigated by site-directed mutagenesis and the crystal structure with its substrate. *J Biol Chem*. 2010;285:20051-20061.
34. Aquino RS, Pereira MS, Vairo BC, et al. Heparins from porcine and bovine intestinal mucosa: are they similar drugs? *Thromb Haemost*. 2010;103:1005-1015.
35. Shriver Z, Sundaram M, Venkataraman G, et al. Cleavage of the antithrombin III binding site in heparin by heparinases and its implication in the generation of low molecular weight heparin. *Proc Natl Acad Sci U S A*. 2000;97:10365-10370.